



**European Union's Seventh Framework Programme
Grant Agreement N°: 603521**

Project Acronym: PREFACE

Project full title: Enhancing prediction of tropical Atlantic climate and its impacts

Instrument: Collaborative Project

Theme: ENV.2013.6.1-1 – *Climate-related ocean processes and combined impacts of multiple stressors on the marine environment*

Start date of project: 1 November 2013

Duration: 48 Months

Deliverable Reference Number and Title:

D 10.1

"Assessment of seasonal to decadal forecast skill in the Tropical Atlantic"

Lead work package for this deliverable: WP10

Lead beneficiary for this deliverable: UiB (Partner 1)

Due date of deliverable: 31.10.2015

Actual submission date: 30.10.2015

Project co-funded by the European Commission within the Seven Framework Programme (2007-2013)		
Dissemination Level		
PU	Public	X
PP	Restricted to other programme participants (including the Commission Services)	
RE	Restricted to a group specified by the Consortium (including the Commission Services)	
CO	Confidential, only for members of the Consortium (including the Commission Services)	

Contribution to project objectives – with this deliverable, the project has contributed to the achievement of the following objectives (see Annex I / DOW, Section B1.1.):

N.º	Objective	Yes	No
1	Reduce uncertainties in our knowledge of the functioning of Tropical Atlantic (TA) climate, particularly climate-related ocean processes (including stratification) and dynamics, coupled ocean, atmosphere, and land interactions; and internal and externally forced climate variability.	X	
2	Better understand the impact of model systematic error and its reduction on seasonal-to-decadal climate predictions and on climate change projections.	X	
3	Improve the simulation and prediction TA climate on seasonal and longer time scales, and contribute to better quantification of climate change impacts in the region.	X	
4	Improve understanding of the cumulative effects of the multiple stressors of climate variability, greenhouse-gas induced climate change (including warming and deoxygenation), and fisheries on marine ecosystems, functional diversity, and ecosystem services (e.g., fisheries) in the TA.		X
5	Assess the socio-economic vulnerabilities and evaluate the resilience of the welfare of West African fishing communities to climate-driven ecosystem shifts and global markets.	X	

Authors of this deliverable:

Noel Keenlyside (lead), Danila Volpi, Eleftheria Exarchou, Chloe Prodhomme, Francisco Doblás-Reyes, Lea Svendsen, Elsa Mohino, Daniel Schönbein, Mao-Lin Shen, Belen Rodríguez-Fonseca, Roberto Suárez-Moreno, Marta Martín-Rey, Irene Polo

Deviation from planned efforts for this deliverable:

There were no significant deviations

Report on the deliverable:

This deliverable is a report on the current forecast skill (anomaly correlation and root mean square error) on s2d and performance of historical coupled climate simulations in the Tropical Atlantic sector, and the performance of statistical forecasts of remote SST anomalies. It is based on tasks 10.5, 10.6, and 10.7.

The first section of the report summarises the skill of seasonal predictions in the tropical Atlantic. The prediction over the North Tropical Atlantic shows significant skill in several seasons. Skill is low in the equatorial and south Atlantic, and in the West African upwelling region and is generally worse than the persistence forecast. However, some models forecasts starting in May, including the ECMWF System4, show high levels of skill for predicting Atlantic equatorial cold tongue anomalies in boreal summer.

The second section provides an assessment of the decadal predictions in the Atlantic Sector. Initialising predictions using contemporary observations is shown to enhance the predictions in the North Tropical Atlantic during the first few years. Model errors likely degrade skill in the South Atlantic. We also show the potential to predict variations the West African monsoon, and that this skill primarily arises from initialisation using contemporary observations. In addition, the forecast of

rainfall for the near future (2016-2019) suggests a positive tendency with respect to the previous four-year period (2011-2014).

Results on extending prediction skill by accounting for low-frequency variations in teleconnections are presented in the third section of the report, and a new statistical model designed to account for these variations is summarised. The model code is freely available. A key result was to show that accounting for the Atlantic impact on the Pacific during the first and last decades of the twentieth century could enhance ENSO prediction. This mechanism may have been active during this year, and contributed to the strong El Niño event in the Pacific that is currently being observed.

The work has led to three peer-review publications (Martín-Rey et al., 2015; Otero et al., 2015; Suárez-Moreno and Rodríguez-Fonseca, 2015), and three more are in preparation.

Forecast quality assessment for the Tropical Atlantic – seasonal timescales

Danila Volpi, Eleftheria Exarchou, Chloe Prodhomme, Francisco Doblado-Reyes, Daniel Schönbein, Mao-Lin Shen, Noel Keenlyside

We have assessed skill of the ECMWF System4 seasonal prediction system and of 14 models from the North American Multi-Model Ensemble (NMME) database (Table 1); and we have assessed the sensitivity of skill to model configuration. We have assessed predictability of tropical Atlantic SST at a grid point level and for indices of selected regions (Table 2) and the four seasons. We have used deterministic skill scores (anomaly correlation and root mean square error (RMSE)). The following summarises key results that will be published in several papers that are currently in preparation.

Table 1: Seasonal prediction experiments from the North American Multi-model Ensemble (NMME) used in this study (<http://www.cpc.ncep.noaa.gov/products/NMME/>). The data were downloaded from <http://iridl.ldeo.columbia.edu/SOURCES/.Models/.NMME/>.

Model	Period	Ensemble size
CMC1-CanCM3	Jan 1981 to Dec 2010	10
CMC2-CanCM4	Jan 1981 to Dec 2010	10
COLA-RSMAS-CCSM3	Jan 1981 to Oct 2015	6
COLA-RSMAS-CCSM4	Jan 1981 to Oct 2015	10
GFDL-CM2p1	Jan 1982 to Feb 2012	10
GFDL-CM2p1-aer04	Jan 1982 to Feb 2015	10
GFDL-CM2p5-FLOR-A06	Mar 1980 to Oct 2015	12
GFDL-CM2p5-FLOR-B01	Mar 1980 to Oct 2015	12
IRI-ECHAM4p5-AnomalyCoupled	Jan 1982 to Jul 2012	12
IRI-ECHAM4p5-DirectCoupled	Jan 1982 to Jul 2012	12
NASA-GMAO	Jan 1981 to May 2012	10
NASA-GMAO-062012	Jan 1981 to Oct 2015	12
NCEP-CFSv1	Jan 1981 to Dec 2009	15
NCEP-CFSv2	Jan 1982 to Dec 2010	24

Table 2: Definition of SST indices

SST index	Region
Equatorial cold tongue (ECT)	20°W-0°, 3°S-3°N
Angola Benguela area (ABA)	20°S-10°S, 8°E-15°E
West African area (WAA)	12°N-25°N, 16°W-20°W
North Tropical Atlantic (NTA)	5°N-20°N, 70°W-20°W
Main development region (MDR)	10°N-14°N, 20°W-70°W

Figure 1 shows the correlation maps for summer (left panel) and winter (right panel) with ERSST data, from 1981 to 2013 obtained from forecast starting respectively in May and November. The lack of skill of the central tropical Atlantic compared to the decadal forecast (below) is reduced and shifted eastward towards the upwelling region of Angola-Benguela; the lack of skill in here is likely related to the large mean model biases in this region. There is a peak of skill in the subtropical North Atlantic, along the coast of Brazil. A second peak of skill is shown in winter in the Gulf of Guinea. Analysis in D9.2 shows the skill close to the Brazilian coast in JJA corresponds arises from the model ability to capture the relatively strong trend.

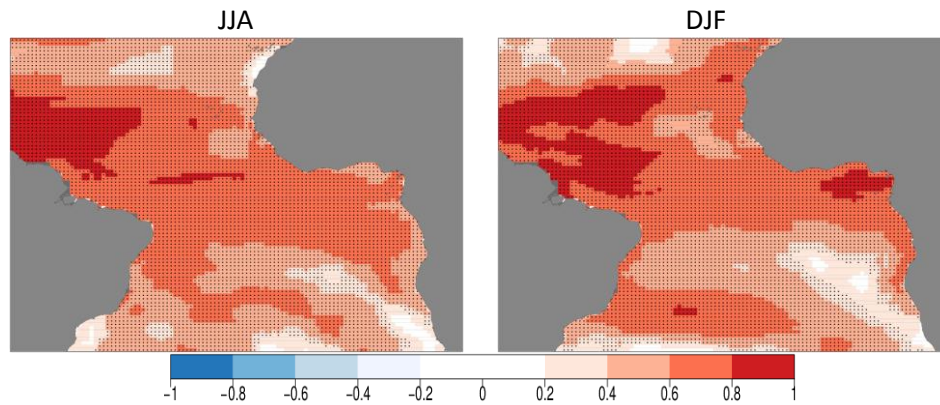


Figure 1: Summer (left panel) and winter (right panel) sea surface temperature anomaly correlation coefficient of System4 with the ERSST data for the period 1981-2013. The black dots indicate the area where the skill is significant with 95% confidence according to a t-test.

The skill of the NMME shows similar characteristics to those shown in Fig. 1 from the ECMWF-System4 predictions, but there is a large intermodel range in prediction skill. For the equatorial cold tongue region, forecasts initiated in February show no skill for JJA when the cold tongue variability peaks (Fig. 2, upper rows). In these forecasts the skill drops rapidly with the majority of models having significantly less skill than the persistence forecast (i.e., the autocorrelation). For forecasts initiated in May, there are five models that show some useful skill for JJA that beats persistence, but still the majority of models perform poorly (Fig. 2, second row). For the Benguela-Angola region, where model errors are particularly large, forecast skill is particularly poor. Forecasts initiated in February for MAM, the season of peak variability, no models show skill beating persistence (Fig. 2, third row).

The skill in the North Tropical Atlantic appears somewhat higher than for the south (Fig. 1), however, persistence skill is also higher. All model forecasts initiated in May for SST averaged over the North Tropical Atlantic region follow the persistence correlation skill closely, but there are several models with better correlation skill and by month 3 RMSE of all models is substantially less than persistence (Fig. 3, top row). In contrast, forecasts started in November show skill beating persistence in terms of both anomaly correlation and RMS error after lead month 3 (Fig 3, middle row). This is consistent with transmission of skill from Pacific via the well-known teleconnection pattern associated with the El Niño Southern Oscillation (ENSO). Unfortunately, this skill drops substantially at the west African Coast, and forecasts started in both May (not shown) and November (Fig 3, bottom row) do not beat persistence in terms of anomaly correlation or RMSE. It may be possible to enhance skill in this region by statistical corrections of the forecasts, as this region is also partly affected by the ENSO teleconnection.

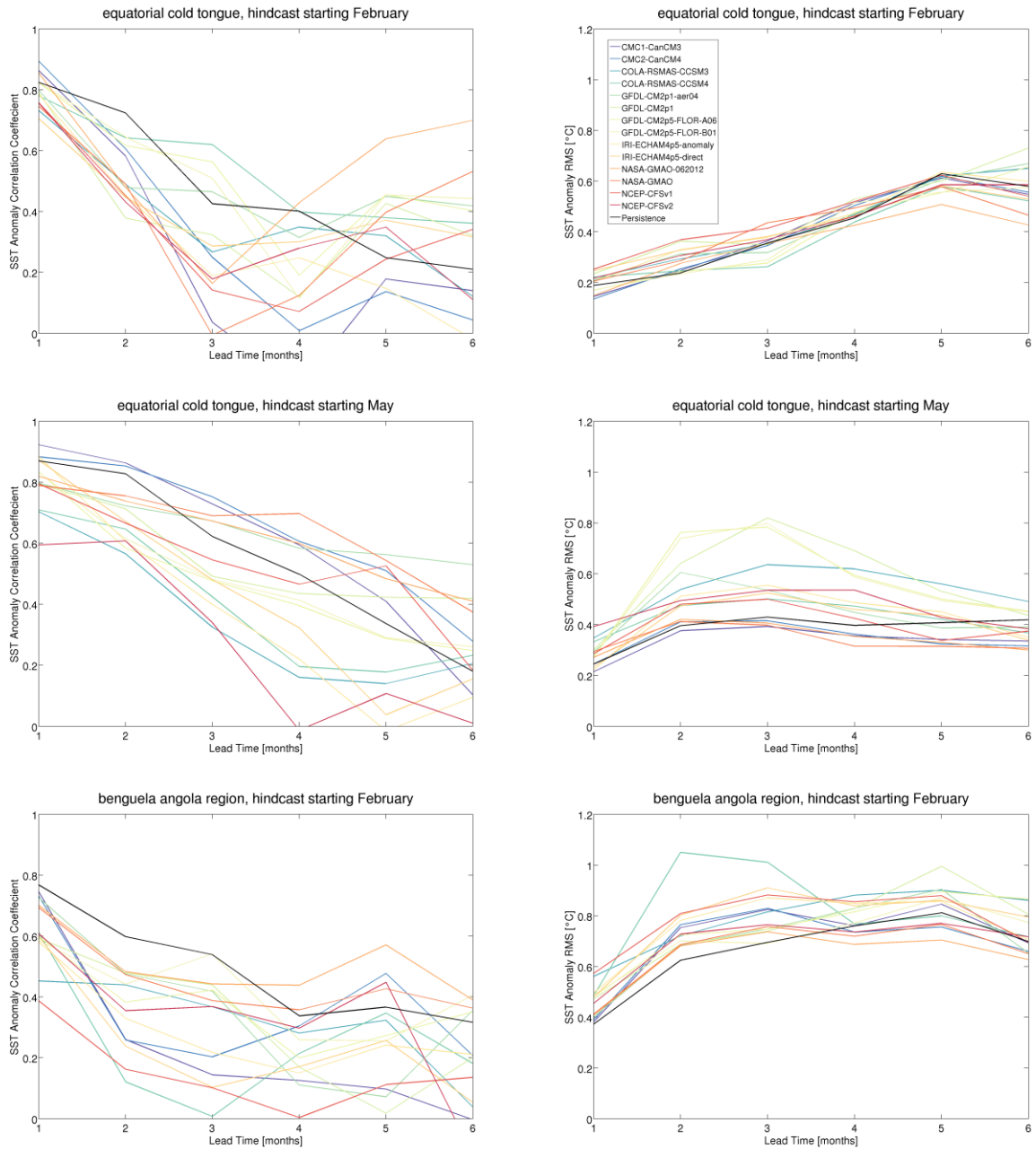


Figure 2: Forecast skill of the NMME in the equatorial and south Atlantic upwelling regions. Anomaly correlation (left) and RMSE (right) skill scores for forecasts of SST in the equatorial cold tongue started in February (upper row) and started in May (middle row), and of the Angola-Benguela area started in February (bottom row). Horizontal axis shows lead-time in months. Scores for individual models are shown in colour and persistence in black.

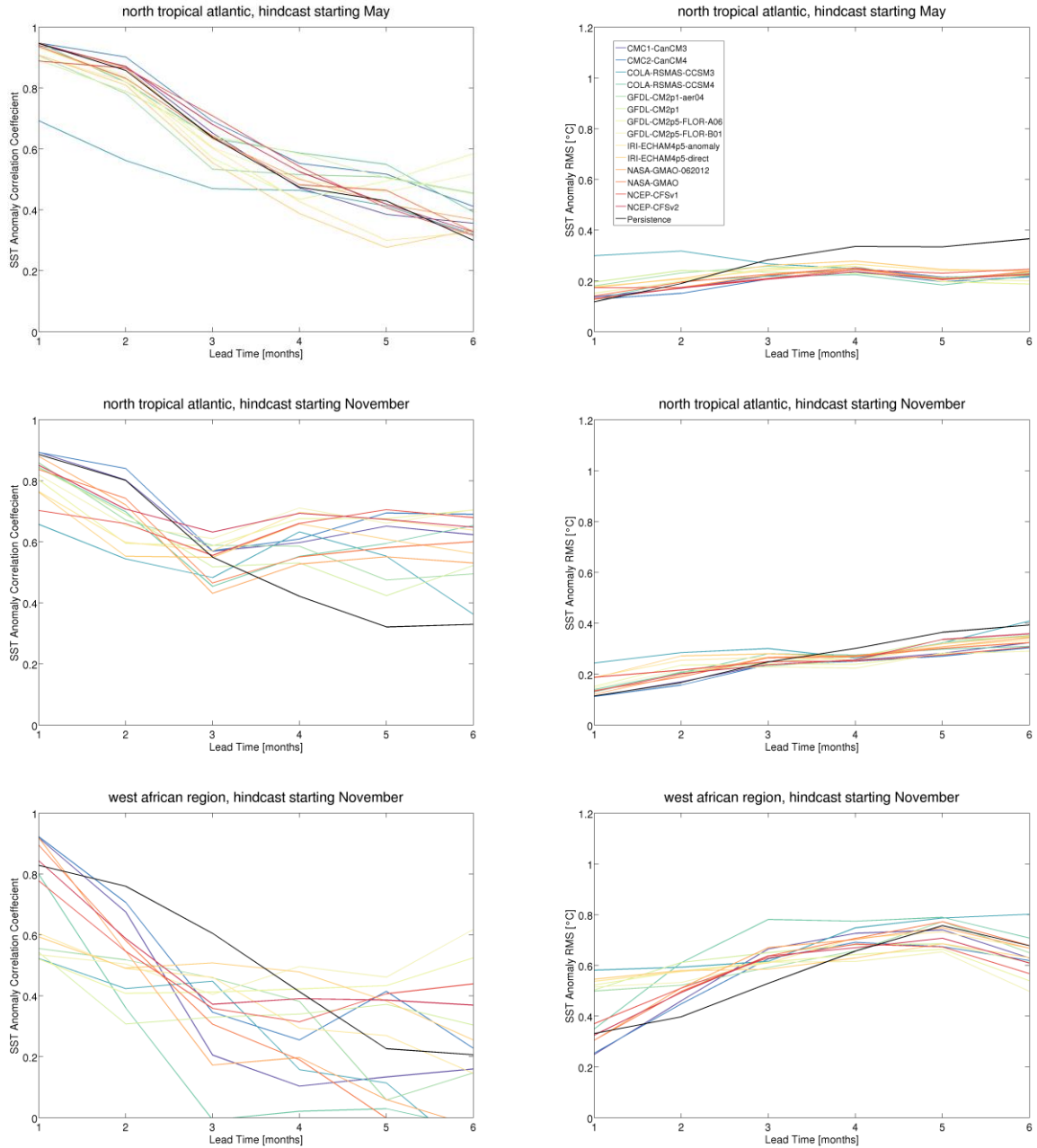


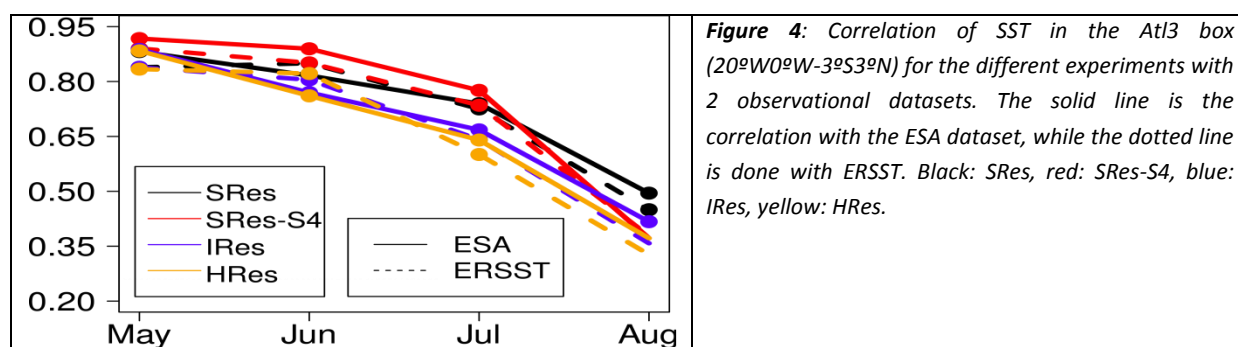
Figure 3: Forecast skill of the NMME in the North Tropical Atlantic and West African upwelling region. Anomaly correlation (left) and RMSE (right) skill scores for forecasts of SST in the North Tropical Atlantic region started in May (upper row) and started in November (middle row), and of the West African region area started in November (bottom row). Horizontal axis shows lead-time in months. Scores for individual models are shown in colour and persistence in black.

We have tested the sensitivity of skill in the region to the resolution increase and change of oceanic initial conditions, using EC-Earth 3.0.1. The experiments are described in Table 3. All the experiments have the atmospheric component initialized with ERA-Interim. One of the standard resolution experiments has the ocean and sea-ice components initialized with ORA-S4 (SRes-S4). All other experiments have the ocean and sea-ice components initialized with GLORYS. We consider both an increase in atmospheric horizontal resolution from T255 to T511 and of oceanic resolution from 1 degree with 46 levels to 0.25 degree with 75 levels.

Table 3: The settings for atmospheric and ocean resolution for sensitivity prediction experiments.

Experiment name	Atmosphere resolution	Ocean resolution	Ocean Initial Condition
SRes	T255L91	ORCA1L46	GLORYS
SRes-S4	T255L91	ORCA1L46	ORA-S4
IRes	T255L91	ORCA025L75	GLORYS
HRes	T511L91	ORCA025L75	GLORYS

Figure 4 shows the sea surface temperature correlation in the Atl3 box (20°W – 0°W – 3°S – 3°N) for the different experiments, calculated against the ESA (solid lines) and ERSST (dotted lines) data. The standard resolution experiment initialized with ORA-S4 has the highest skill during the first month of the hindcast. The reason for which the hindcasts initialised with GLORYS performs worse than the ones initialised with ORA-S4 could probably be related to GLORYS strong surface and subsurface biases in temperature and salinity in the Atlantic 3 region during some years. Moreover we see that increasing the oceanic and atmospheric resolution degrades the skill in the region. This is probably due to the fact that the high-resolution version of the model is less tuned than the standard resolution.



Forecast quality assessment for the Tropical Atlantic – Decadal timescales

Danila Volpi, Eleftheria Exarchou, Chloe Prodhomme, Francisco Doblaz-Reyes, Lea Svendsen, Elsa Mohino, Noel Keenlyside

We have performed a systematic analysis of the forecast skill in the tropical Atlantic on decadal timescales by using historical and decadal prediction experiments from CMIP5 (Taylor et al., 2008) and the EU SPECS project (<http://www.specs-fp7.eu>). Our results highlight the role of internal climate dynamics in driving North Atlantic decadal variability, and show that climate predictions initialised from contemporary observations can skilfully predict North Atlantic SST and Sahel Rainfall. A paper on the later has been published (Otero et al., 2015). The mechanisms controlling Tropical Atlantic decadal variability and its teleconnection mechanisms are further discussed in D9.2.

We analyse historical simulations from 20 CMIP5 models for their ability to reproduce the observed variations in North Atlantic SST for three different indices: The Atlantic multi-decadal variability (AMV) index (defined as SST averaged from 0-60°N in the Atlantic, with the linear trend, removed, and smoothed with an 11 year running mean), and its tropical (0-30°N) and extra-tropical (30-60°N) constituents. These models, driven only with historical forcing, do not reproduce decadal variations in North Atlantic SST (Fig. 5, Tab. 4); this is consistent with previous studies (Kavvada et al., 2013; Medhaug and Furevik, 2011; Ting et al., 2009). The average correlation between observed and simulated variations for the 20 CMIP5 models is around 0.3, which is not statistically significant at the 90% level ($r \sim 0.58$). Only the BCC-CSM1-1 model simulation has a marginally significant correlation of 0.58. The agreement between model and observations is even poorer when considering tropical and extra-tropical SST variations, separately (Table 4). Thus, SST variations in both regions likely result from internal climate dynamics (See also Deliverable 9.2).

To see if initialisation can lead to better predictions of Atlantic SST variations, we compare predictions driven with historical radiative forcing and initialised using contemporary observations to simulations driven by only historical radiative forcing (Table 5). Each decadal prediction experiment consists of a set of predictions initialized every year on the 1st of January over a different period (see third column in Table 5 for details). Every member available for each experiment has been used, which means that chaotic noise has been filtered out more efficiently in systems having more members. The analysis is carried out on the original grid of each experiment to reduce the impact of the interpolation.

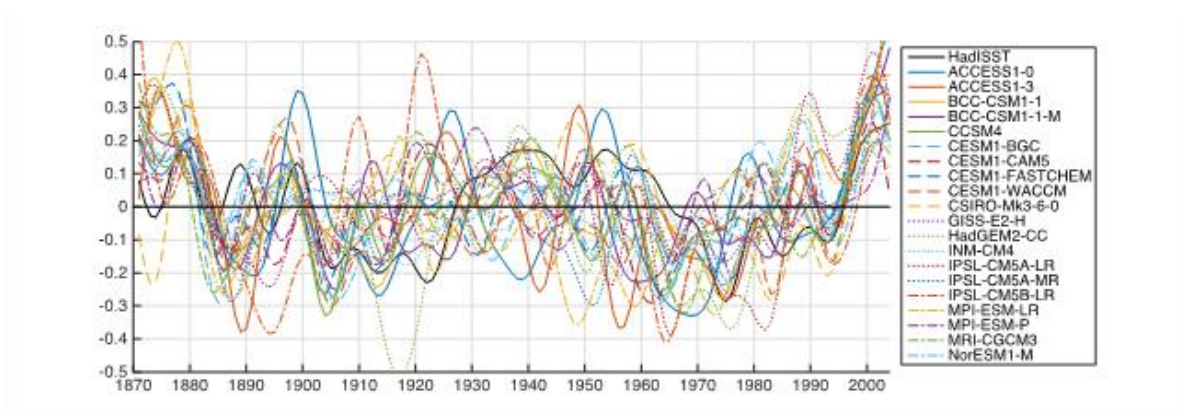


Figure 5. The observed AMV index (black) and simulated by 20 CMIP5 models with historical forcing (thin coloured lines).

Table 4: Correlation skill of CMIP5 models in reproducing observed SST variations over three different regions of the North Atlantic. All indices have been smoothed with an 11-yr running mean and the linear trends have been removed. For 9 degrees of freedom the 95% significance level for a two-sided test is 0.66, and the 90% level is 0.58.

CMIP5 model	Index region		
	0-60°N	0-30°N	30-60°N
ACCESS1-0	0,40	0,15	0,43
ACCESS1-3	0,22	0,19	0,07
BCC-CSM1-1	0,58	0,49	0,44
BCC-CSM1-1-M	0,45	0,37	0,41
CCSM4	0,37	0,25	0,32
CESM1-BGC	0,27	0,24	0,09
CESM1-CAM5	0,13	0,14	0,01
CESM1-FASTCHEM	0,45	0,25	0,42
CESM1-WACCM	0,27	0,30	0,26
CSIRO-Mk3-6-0	0,57	0,39	0,46
GISS-E2-H	0,54	0,21	0,44
HadGEM2-CC	0,45	0,34	0,37
INM-CM4	0,22	0,23	0,24
IPSL-CM5A-LR	0,40	0,19	0,34
IPSL-CM5A-MR	0,35	0,41	0,29
IPSL-CM5B-LR	0,14	0,00	0,00
MPI-ESM-LR	-0,16	0,06	-0,32
MPI-ESM-P	0,21	0,41	-0,14
MRI-CGCM3	0,33	0,17	0,26
NorESM1-M	0,40	0,32	0,37
Mean	0,33	0,25	0,24
Max	0,58	0,49	0,46
Min	-0,16	0,00	-0,32

Table 5: CMIP5 and SPECS decadal experiments used, with the number of members and the covered period.

Model	No. members init prediction	No. members historical	Period (1 start date per year)
MIROC5	6	1	1961-2011
HadCM3	10	10	1961-2010
EC-Earth v2.3	5	10	1961-2006
MPI (SPECS decadal)	5	3	1961-2012
GFDL-CM2	10	10	1961-2012
CANCM4	10	10	1961-2012

Figure 6 shows the anomaly correlation maps of the different experiments with ERSST data (see Garcia-Serrano and Doblas-Reyes, 2012 for a description of the methodology) respectively for the first forecast year (first row), the average over years 2 to 5 (second row) and 6 to 9 (third row). There is a general lack of skill in the southern central tropical Atlantic and along the Angola-Benguela area (ABA), which is a region of strong bias. The region with highest skill during the first forecast year is the subtropical North Atlantic for all models except for MPI, which exhibits a lack of skill close to the Mauritanian coast.

Figure 7 shows the analogous skill maps produced with the respective historical simulations. All historical simulations have lower skill than the initialized experiment during forecast year 1. However, for the following forecast years the models have different behaviours: while the initialized experiment of MIROC5 has slightly higher skill than its historical counterpart in the subtropical North Atlantic during the years 2-5 and 6-9, HadCM3, EC-Earth 2.3, GFDL and CANCM4 do not show better forecast skill than the respective historical simulations during those years. This supports the idea that the skill for the following forecast years is mainly given by the long-term trend, which means that for those systems the sensitivity to the initial conditions in the region is not significant after forecast year 1. Only MPI exhibits better skill with initialization along the Mauritania coast during the whole forecast period. Further analysis is provided in D9.2 on the role of trend versus variability about the trend in these simulations.

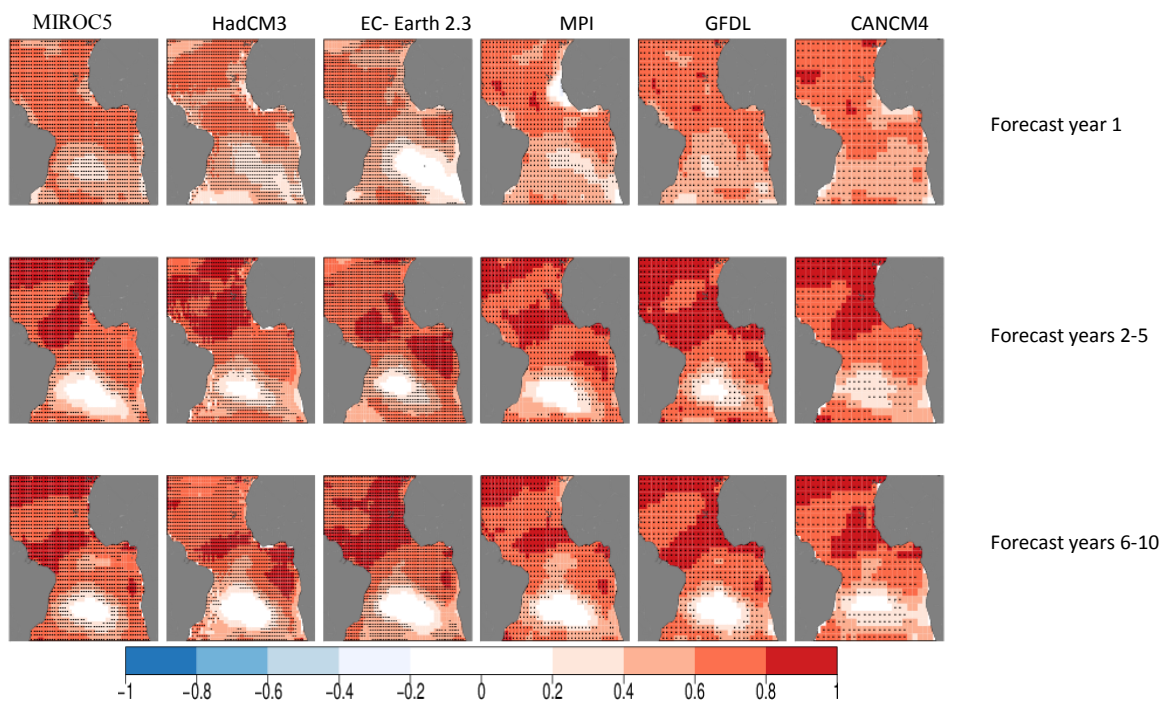


Figure 6: Sea surface temperature anomaly correlation coefficient of some decadal initialized CMIP5 and SPECS experiments, with the ERSST data. The columns represent respectively MIROC5, HadCM3, EC-Earth 2.3, MPI, GFDL and CANCM4 models. The reference period changes depending on the availability of the prediction data (see table 1). First row shows forecast year 1, second row the average over forecast years 2 to 5 and the third row the average over the years 6 to 9. The black dots indicate the areas where the skill is significant with 95% confidence according to a t-test.

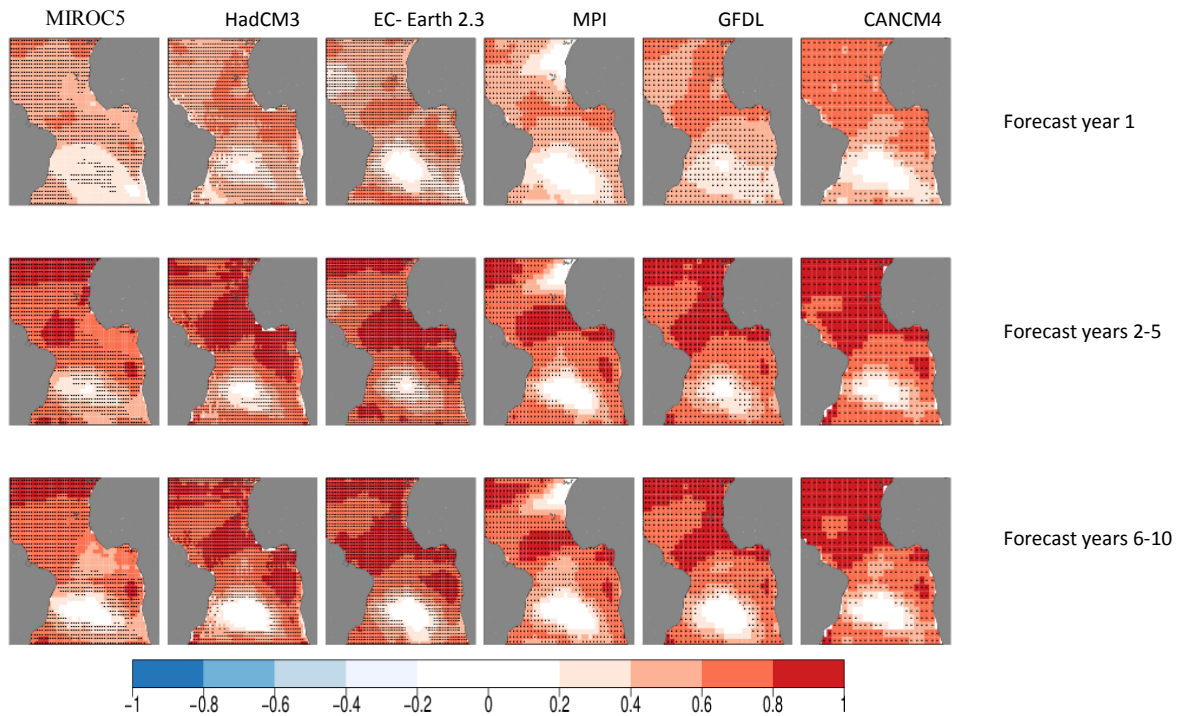


Figure 7: Sea surface temperature anomaly correlation coefficient of some decadal historical CMIP5 and SPECS simulations, with the ERSST data. The columns represent respectively MIROC5, HadCM3, EC-Earth 2.3, MPI, GFDL and CANCM4 models. The reference period changes depending on the availability of the data of the respective initialized experiment (see table 1). First row shows forecast year 1, second row the average of forecast years 2 to 5 and third row the average of the years 6 to 9. The black dots indicate the area where the skill is significant with 95% confidence according to a t-test.

Lastly, we assess the capability of state-of-the-art coupled climate models in predicting the precipitation in Sahel at decadal time scales, and identify the skill arising from initialisation versus radiative forcing (these results were published in Otero et al., 2015). The Sahel region has shown prominent fluctuations in rainfall at decadal time scales associated with SST variability. The skill of 13 models participating in CMIP5 in forecasting Sahel rainfall at decadal time scales was assessed in two different experiments: initialised decadal hindcasts and forced historical simulations. Considering the strong linkage of the atmospheric circulation signatures over West Africa with the rainfall variability, we have investigated the potential of using the dynamic-based West African monsoon index (WAMI), which accounts for the intensity of the monsoonal circulation. The WAMI is based on the coherence of low (925 hPa) and high (200 hPa) troposphere wind fields and is defined following a combined empirical orthogonal functions (CEOF) analysis.

WAMI from coupled models is compared with a standardised precipitation index (SPI) from observations to assess predictive skill. Several models indicate skill in predicting SPI, but the skill is highly model-dependent, is strongly related to the region chosen for the WAMI definition, and depends on lead-time (Fig. 8). In addition, hindcasts are more skilful than historical simulations, suggesting an added value of initialisation for decadal predictability. In further support of this, the models are skilful in predicting variability about the externally-forced component of climate variability (computed by a signal-to-noise maximising technique).

The skill in predicting WAMI from reanalysis products was also assessed. The results showed the models had comparable skill in predicting WAMI from the NECP reanalysis, but could not predict

variations in the ERA40 likely due to deficiencies in this region of the reanalysis (not shown). In some models, the WAMI yields improved skill with respect to the direct rainfall outputs. Therefore, dynamic-based indices are potentially more effective for decadal prediction of precipitation in Sahel than precipitation-based indices for those models in which Sahel rainfall variability is not well simulated. Thus a twofold approach is recommended when testing the performance of models in predicting Sahel rainfall, based not only on rainfall but also on the dynamics of the West African monsoon.

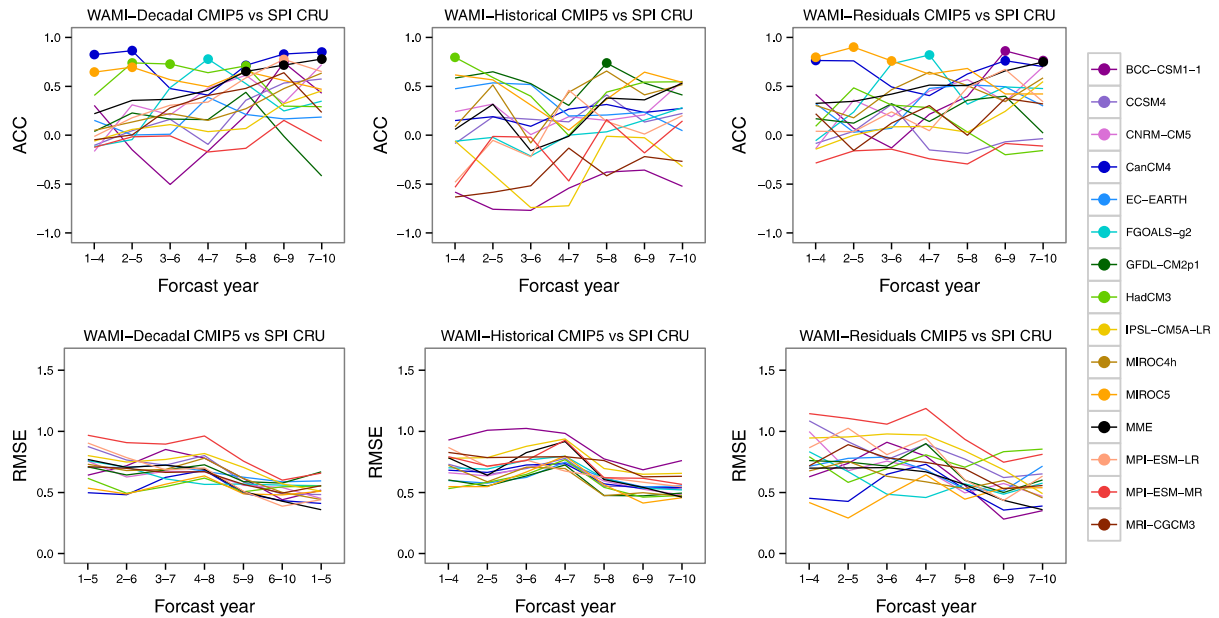


Figure 8: Anomaly correlation coefficient (ACC) (top) and RMSE (bottom) skill scores for modelled WAMI in decadal hindcasts (left), historical experiment (middle) and decadal-forcing residuals (right), tested against the Sahel precipitation index (SPI) from CRU data. Dots indicate significant ACC at 95 % level of confidence. The figure is from Otero et al. 2015.

In Fig. 9 we show the multidecadal variability of observed precipitation along with the WAMI simulated in the decadal hindcasts. Standardised anomalies of SPI are computed for the CRU dataset until 2009 and GPCP dataset up to 2014. In this plot, we show the results for the 6–9 years lead-time, since the skill of prediction for the models has been detected mostly at long lead times (Fig. 8). Standardized anomalies of the indices are computed averaging the WAMI for several multi-model ensembles: a multimodel mean for all models from the decadal hindcasts (MME); a mean for the most skilful models in our analysis (MMEsk). A subset of only 6 models is considered for the future outlook (MME6), as not all models provided the decadal simulation initialized in 2010; and we also consider an ensemble of the 4 most skilful of these (MME6sk). The climate predictions are able to capture the low frequencies variations, including the dry period in the 1980’s. In addition, the forecast of rainfall for the near future (2016-2019) suggests a positive tendency with respect to the previous four-year period (2011-2014) (Fig. 9).

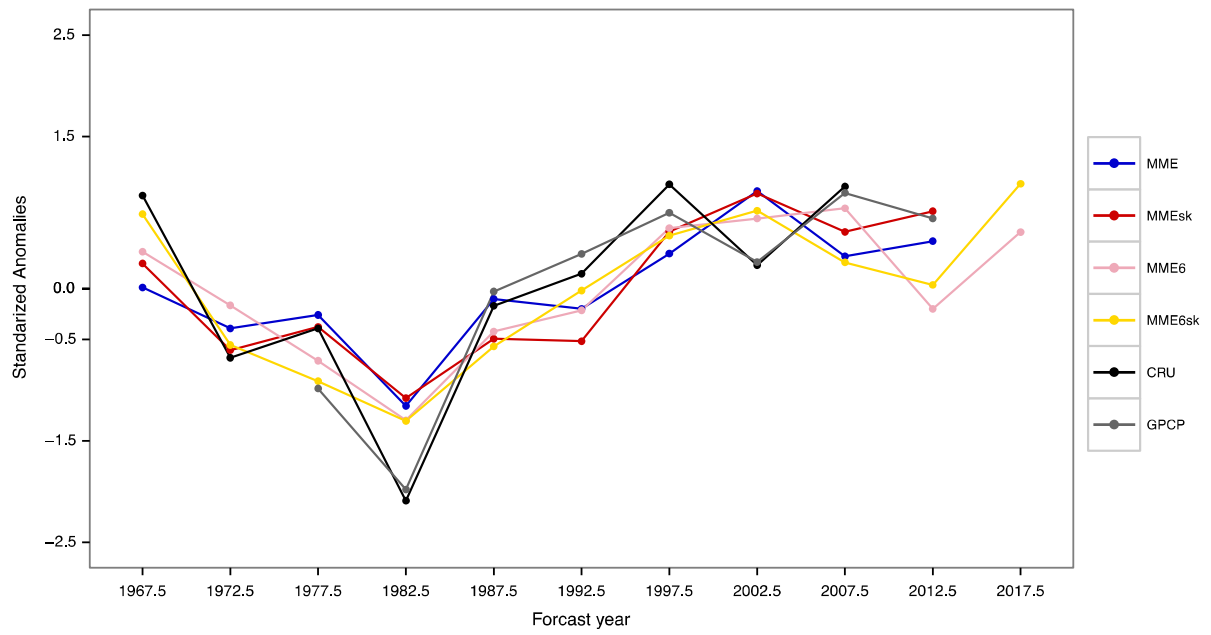


Figure 9: Standardised anomalies of the observed SPI from CRU and GPCP datasets, and multi-model ensemble mean WAMI computed for all (MME) and skilful (MMEsk) models available up to the 2006-2015 decade, and for all (MME6) and skilful (MME6sk) models available up to the 2011-2020 decade. The figure is from Otero et al. 2015.

The performance of statistical forecasts of remote SST anomalies

Belen Rodríguez-Fonseca, Roberto Suárez-Moreno, Marta Martín-Rey, Irene Polo

It is becoming accepted that interannual teleconnections may be modulated by low-frequencies modes of climate variability, such as the AMV (López-Parages and Rodríguez-Fonseca, 2012) or the Interdecadal Pacific Oscillation (Power et al., 1999). Here we investigate the potential of capturing predictability associated with the modulation of teleconnections. First we show that by capturing the multi-decadal modulation teleconnections from the Atlantic to the Pacific (Ding et al., 2012; Martín-Rey et al., 2014; Rodríguez-Fonseca et al., 2009) ENSO prediction can be enhanced during periods when the teleconnection is strong. Second, we develop a generalised statistical prediction model that can account for the low-frequency modulation of teleconnections. Two papers were published on these results (Martín-Rey et al., 2015; Suárez-Moreno and Rodríguez-Fonseca, 2015).

It was recently shown that an Atlantic Niño (Niña) tend to precede Pacific Niña (Niño) during the first and last decades of the twentieth century (Martín-Rey et al., 2014). During these decades, the Atlantic influences the Pacific through perturbations to the Walker Circulation that are then enhanced by ocean-atmosphere interaction in the Pacific (Ding et al., 2012; Rodríguez-Fonseca et al., 2009). Here a statistical cross-validated hindcast of ENSO along the twentieth century is presented, considering the Atlantic sea surface temperatures as the unique predictor field, and a set of atmospheric and oceanic variables related to the Atlantic-Pacific connection as the predictand field.

The observed ENSO phase is well reproduced, and the skill is enhanced at the beginning and the end of the twentieth century (Fig. 10). The correlation maps between the observed and predicted tropical Pacific variables involved in ENSO development (SST, zonal wind stress, and z20) reveal a high-prediction skill at the beginning of the twentieth century and also after the late 1960s. In particular, an agreement between the observed and cross-validated zonal wind stress is shown in western Pacific (120°E–160°W; 15°N–15°S), reaching correlation scores of 0.4–0.6. The perturbation of the thermocline depth in the central Pacific (180°–130°W, 5°N–5°S) during JASO season is also well reproduced by the hindcast, with correlation scores of 0.4 (Figures 10d and 10f). Finally, the model describes the eastward and westward propagation of z20 anomalies reflecting the Bjerknes positive feedback (Figures 10g and 10i). Finally, the hindcast reproduces an ENSO-like pattern during DJFM season, characterized by the central-eastern equatorial tongue (Figures 10j and 10l). On the contrary, for the period 1939–1966 (Figures 10b, e, h, k), no significant correlation scores are found between observed and predicted tropical Pacific variables; thus, there is no ENSO predictability from the Atlantic SST during this period of time. Understanding this multidecadal modulation of the Atlantic-Pacific connection could help to improve seasonal-to-decadal forecasts of ENSO and its associated impacts.

The SST based Statistical Seasonal Forecast Model (S4CAST; Suárez-Moreno and Rodríguez-Fonseca, 2015) has been developed in order to evaluate and quantify the predictability of climate-related variables susceptible to be influenced by SST. The model is intended as a medium-range to long-range prediction tool and allows the user to enter a series of input parameters in a simple and intuitive way. It is based on Maximum Covariance Analysis and analyses the relationship between the predictor and the predicted time series in order to consider non-stationary connections between both fields. Thus, changes in predictability over a study period can be considered to improve

operational predictions provided by dynamical models. The model has been first applied to study the predictability of Sahel rainfall and is currently being applied to study the remote influence from tropical Atlantic. The model consists of a software package organized in folders containing libraries, functions and scripts developed as a MATLAB toolbox from version R2010b onwards. The code is Open Access and can be downloaded from the Zenodo repository (DOI 10.5281/zenodo.15985) in the URL <https://zenodo.org/record/15985>.

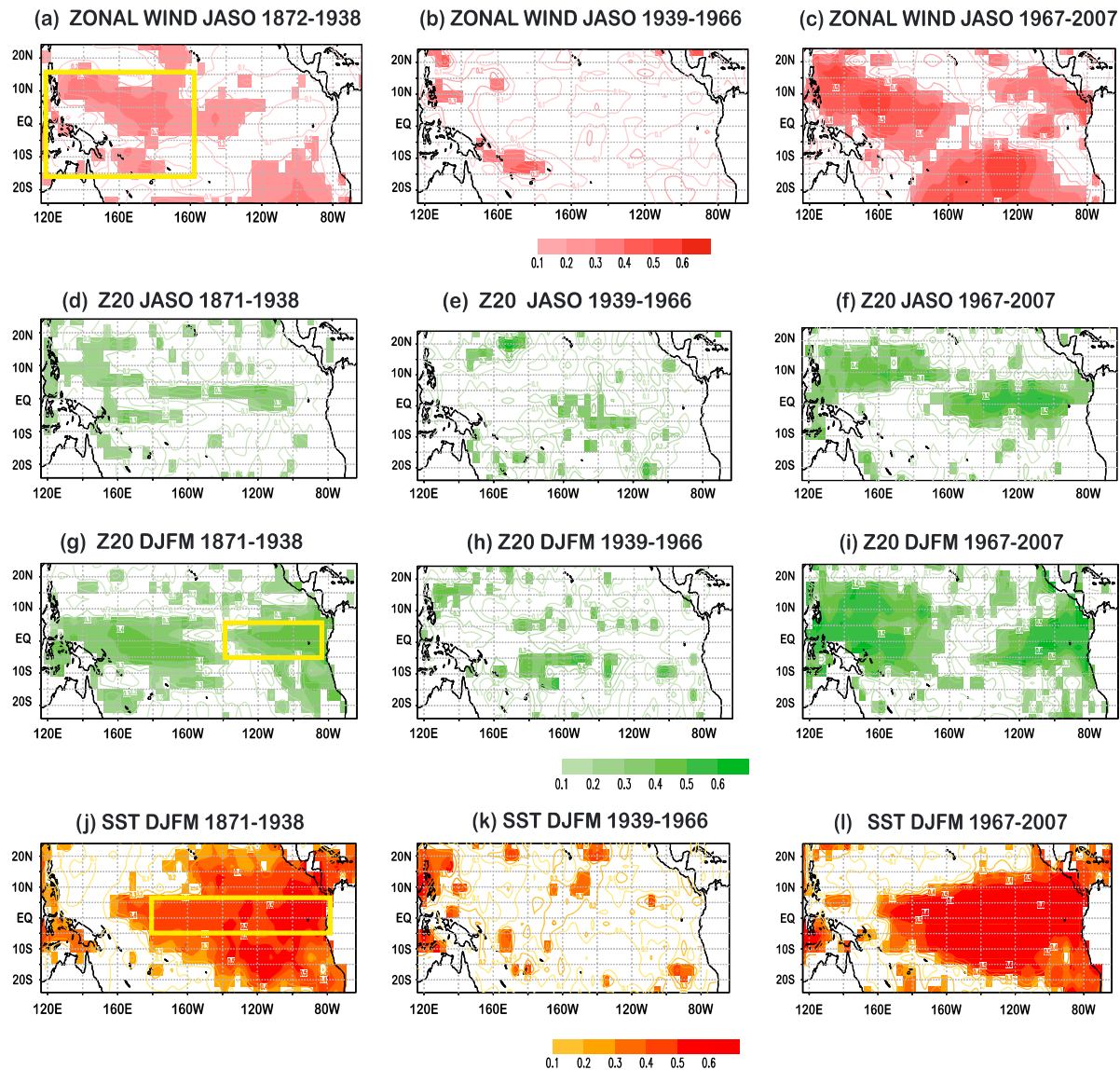


Figure 10: Correlation maps between observed and predicted variables over tropical Pacific. Correlation maps between the observed and predicted zonal wind stress in (a–c) JASO, (d–i) JASO–DJFM thermocline depth, and (j–l) DJFM SST; for the periods 1871–1938 (a, d, g, and j), 1939–1966 (b, e, h, and k), and 1967–2007 (c, f, i, and l). Significant values exceeding 90% confidence level according to a Monte Carlo test are presented in shaded. Figure from Martín-Rey et al., 2015.

References

PREFACE contributions in blue.

- Ding, H., N. Keenlyside, and M. Latif, 2012: Impact of the Equatorial Atlantic on the El Niño Southern Oscillation. *Climate Dynamics*, **38**, 1965-1972.
- García-Serrano, J. and F.J. Doblas-Reyes (2012). On the assessment of near-surface global temperature and North Atlantic multi-decadal variability in the ENSEMBLES decadal hindcast. *Climate Dynamics*, 39, 2025-2040, doi: 10.1007/s00382-012-1413-1.
- Kavvada, A., A. Ruiz-Barradas, and S. Nigam, 2013: AMO's structure and climate footprint in observations and IPCC AR5 climate simulations. *Climate Dynamics*, **41**, 1345-1364.
- López-Parages, J. and B. Rodríguez-Fonseca, 2012: Multidecadal modulation of El Niño influence on the Euro-Mediterranean rainfall. *Geophysical Research Letters*, **39**, L02704.
- Martín-Rey, M., B. Rodríguez-Fonseca, I. Polo, and F. Kucharski, 2014: On the Atlantic–Pacific Niños connection: a multidecadal modulated mode. *Climate Dynamics*, **43**, 3163-3178.
- Martín-Rey, M., B. Rodríguez-Fonseca, and I. Polo, 2015: Atlantic opportunities for ENSO prediction. *Geophysical Research Letters*, **42**, 6802-6810.
- Medhaug, I. and T. Furevik, 2011: North Atlantic 20th century multidecadal variability in coupled climate models: sea surface temperature and ocean overturning circulation. *Ocean Sci. Discuss.*, **8**, 353-396.
- Otero, N., E. Mohino, and M. Gaetani, 2015: Decadal prediction of Sahel rainfall using dynamics-based indices. *Climate Dynamics*, 1-17.
- Power, S., T. Casey, C. Folland, A. Colman, and V. Mehta, 1999: Inter-decadal modulation of the impact of ENSO on Australia. *Climate Dynamics*, **15**, 319-324.
- Rodríguez-Fonseca, B., I. Polo, J. Garcia-Serrano, T. Losada, E. Mohino, C. R. Mechoso, and F. Kucharski, 2009: Are Atlantic Niños enhancing Pacific ENSO events in recent decades? *Geophysical Research Letters*, **36**, L20705.
- Suárez-Moreno, R. and B. Rodríguez-Fonseca, 2015: S4CAST v2.0: sea surface temperature based statistical seasonal forecast model. *Geosci. Model Dev. Discuss.*, **8**, 3971-4018.
- Taylor, K. E., R. J. Stouffer, and G. A. Meehl, 2008: A summary of the CMIP5 Experimental Design. <http://www-pcmdi.llnl.gov/>.
- Ting, M. F., Y. Kushnir, R. Seager, and C. H. Li, 2009: Forced and Internal Twentieth-Century SST Trends in the North Atlantic. *Journal of Climate*, **22**, 1469-1481.